

# Very Fast Metal–Semiconductor–Metal Ultraviolet Photodiodes on GaN with Submicron Finger Width

Metal–semiconductor–metal (MSM) photodiodes made on GaN are attractive candidates for fast ultraviolet (UV) signals due to the simplicity of fabrication and the visible blind feature (no response for  $\lambda > 365$  nm). The temporal response of a MSM photodetector fabricated on GaN has been examined both theoretically<sup>1</sup> and experimentally.<sup>2–4</sup> While the theoretical modeling for a 0.25- $\mu\text{m}$  MSM interdigitated structure predicted a small time constant of 3.5 ps, experimental measurements have been limited to feature dimensions no smaller than 2  $\mu\text{m}$ . More recently T. Palacios *et al.*<sup>5</sup> reported on the responsivity of submicron (0.5- $\mu\text{m}$ ) MSM UV detectors on GaN; however, the temporal response was not characterized. In this article, we present the results of temporal measurements of a MSM photodiode on GaN with finger width and pitch ranging from 0.3  $\mu\text{m}$  to 5  $\mu\text{m}$ . These detectors were packaged with a specially designed fast circuit. The minimum temporal resolution between consecutive optical pulses was measured to be 26 ps. At high illumination levels, broadening of the detector response was observed and can be attributed to space-charge screening.

The GaN wafers (2- $\mu\text{m}$  thickness) grown on *c*-plane sapphire were purchased from Technologies and Devices International, Inc.<sup>6</sup> The residual impurities produced a free-electron concentration below  $1 \times 10^{16} \text{ cm}^{-3}$ . The MSM detectors were fabricated at Cornell Nanofabrication Facilities (CNF) using electron-beam lithography. A 15-nm Au layer was deposited prior to the exposure of the electron beam due to the low conductivity of the material. Native oxide on the surface was removed with a diluted HF (hydrofluoric acid) solution prior to metallization, Ti/Pt (5 nm/80 nm). The finger spacing and width, which were equal, ranged from 0.3  $\mu\text{m}$  to 5  $\mu\text{m}$ . The active area was either  $50 \times 50 \mu\text{m}^2$  or  $25 \times 25 \mu\text{m}^2$ . After fabrication of the fingers, a FOx-12 (field oxide) negative resist layer with 450-nm thickness was deposited and exposed with the *e* beam to form a  $\text{SiO}_2$  passivation layer over the entire device.

Unlike other high-speed measurements that used microwave techniques,<sup>7,8</sup> our time-domain experiments used a

broadband circuit to directly couple out the electrical pulse generated in the active area. The top view of this fixture is shown in Fig. 93.38. The backside of the circuit board is grounded. The transmission line width was designed to be 1.1 mm to match the 50- $\Omega$  impedance of the 34-GHz digitizing oscilloscope. A large bias resistor  $R_c$  was used to block out reflections from the charging circuit. To avoid an abrupt width change, a pad with a curved taper, calculated<sup>9</sup> to reduce the impedance mismatch between the transmission line and the active area, was fabricated on the device. An ultrabroadband (12 KHz to 40+ GHz) optical capacitor (“Opt-Cap” in Fig. 93.38) is soldered on the edge of the board to produce a high-speed electrical connection to the backside ground plane. The sample is glued on the gap between the transmission line and the Opt-Cap and electrically connected by silver paste. The impulse response of the whole detector was simulated numerically.<sup>10</sup>

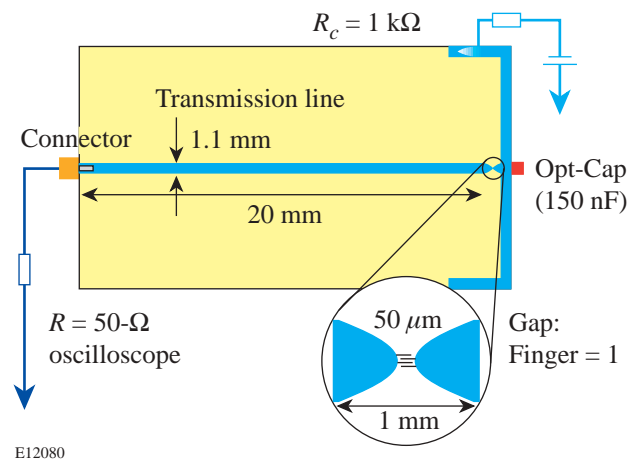


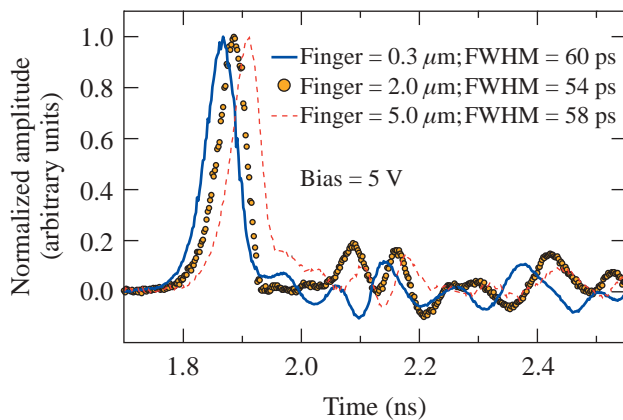
Figure 93.38

Top view of the broadband circuit designed for the MSM photodiode.  $R_c$  (1 k $\Omega$ ) isolates the electrical pulse from bias circuit. An ultrabroadband optical capacitor (Opt-Cap) was soldered to the device and the ground. To avoid an abrupt width change, a pad with a calculated curve tapers the transmission line down to the active area.

The temporal response measurement was implemented with a mode-locked Ti:sapphire laser ( $\lambda \sim 810$  nm). The output of the femtosecond laser was coupled into a custom-built third-harmonic generator to produce a UV beam ( $\lambda \sim 270$  nm). The beam was then focused onto the active area of the sample by a UV-grade fused-silica lens with a 2-cm focal length. The focal spot was measured to be smaller than  $10 \mu\text{m}$ . The electrical pulse was displayed on a 34-GHz digital oscilloscope and recorded by a computer.

The device was plugged directly into the oscilloscope to eliminate the dispersion from connecting cables. Figure 93.39 is a plot of the normalized signal from devices with different fingers widths ( $0.3 \mu\text{m}$ ,  $2 \mu\text{m}$ , and  $5 \mu\text{m}$ ) under 5-V bias. The curves have been shifted in time for visual convenience. The optical energy is about 6 pJ/pulse. The main peaks are followed by ringing reflections from the circuit. It is interesting to compare our data on the  $5 \mu\text{m}$  with those in Ref. 2: they reported a full width at half maximum (FWHM) of longer than 100 ps at 5-V bias, almost twice the pulse duration we measured. The slower response was attributed<sup>2</sup> to carrier transit time, which is contradicted by our experiments.

Further, our data show that the fall time is even faster than the rise time for all the samples at low illumination level, and the FWHM's of the impulse response from different fingers (60 ps for  $0.3 \mu\text{m}$ , 54 ps for  $2 \mu\text{m}$ , and 58 ps for  $5 \mu\text{m}$ ) are similar (Fig. 93.39).



E12081

Figure 93.39 Time response of the detectors with different fingers ( $0.3 \mu\text{m}$ ,  $2 \mu\text{m}$ , and  $5 \mu\text{m}$ ) under 5-V bias. The amplitudes of the signal have been normalized to the peak values, and the dc background has been subtracted.

To study the relationship between electric field and temporal response time, we changed the bias voltage from 1 V to 10 V while maintaining the same illumination level. The pulse durations remained essentially the same. Another sample, with a  $0.3\text{-}\mu\text{m}$  finger spacing and a  $25 \times 25\text{-}\mu\text{m}^2$  active area, was examined. Its FWHM was measured at 58 ps, almost the same as the larger samples, thus eliminating device capacitance as the dominant factor contributing to the pulse width. This led us to examine the measurement test fixture, including the silver paste, the discontinuity of the connector, the surface roughness, and the width variation of the transmission line. The combined effect could cause the charging and discharging of the device to experience different impedances. For the device with  $0.3 \mu\text{m}$ , using reflection (ringing) in the response signal, which is 12% of the peak, we estimate the discharging impedance to be  $63 \Omega$ . If the charging time is determined by the  $Z_C = 63 \Omega$  and discharging time is determined by oscilloscope impedance,  $50 \Omega$ , the ratio of them should be  $63:50 = 1.26$ . This matches well with the experimental results of 58-ps rise time and 45-ps fall time. Overall we believe that at a low illumination level the very short electrical pulse generated in our detectors was broadened by the measurement system and the real impulse response of the samples should be faster than the measured pulse duration.

To explore further the inherent device response, a split-beam technique was used. In these experiments, the UV beam was split into two parts with an adjustable delay. The two pulses were then used to excite the detector. Figure 93.40 shows the results of the double-pulse measurement for a device with  $0.3\text{-}\mu\text{m}$  finger and  $25 \times 25\text{-}\mu\text{m}^2$  active area at 5-V bias. Separable responses began to be discernible at a time delay of 26 ps. This indicates that our devices had an inherent response time of less than 26 ps. When one optical pulse was delayed by 54 ps, the two pulses were well resolved: the value of the valley was about 70% of the value of the peak. This is consistent with our measured pulse duration. If delayed further to 90 ps, the two pulses were clearly separated, as can be seen in the plot.

The power dependence of the response speed was studied by tuning the UV output from the custom-built tripling system from 3 pJ to 391 pJ. In Fig. 93.41 we plot the temporal response data of a sample with  $0.3\text{-}\mu\text{m}$  finger width for optical pulse energies of 3, 116, and 391 pJ, respectively. Again the signal amplitudes have been normalized to their peak values. The applied bias is 5 V for all measurements. As the incident optical energy increases, the rise time remains almost constant; however, the fall time increases significantly. This is attributed

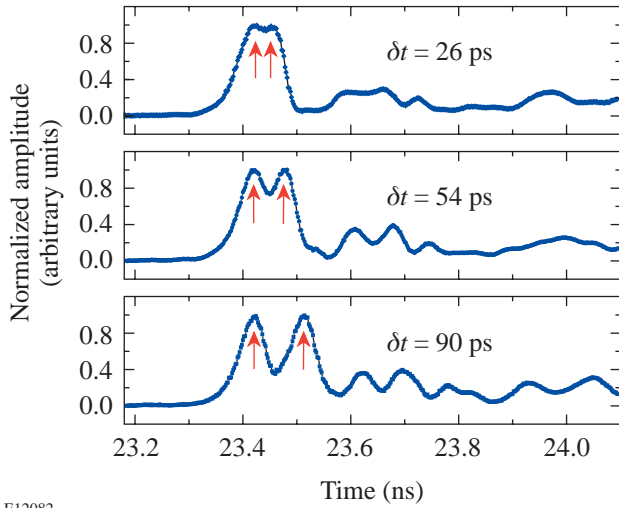


Figure 93.40 Time resolution of the detector in free space. The beam was split into two parts, and one of them was delayed. When the delay was 26 ps, two main peaks started to be discernable. The reflections of the circuit can also be clearly seen.

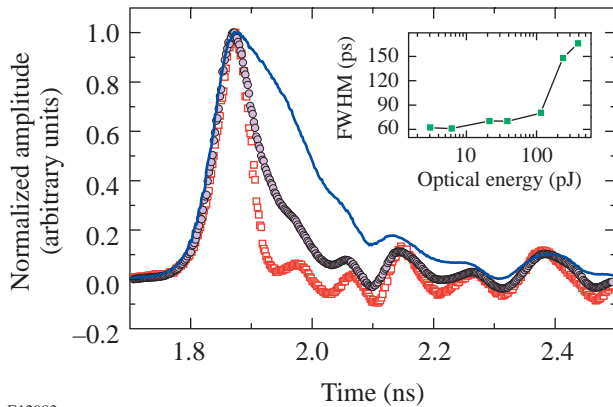


Figure 93.41 Impulse response of MSM devices under different illumination energies of 3 pJ (squares), 116 pJ (circles), and 391 pJ (solid line). The insert shows the dependence of pulse width on the incident optical energy. The pulse duration remains constant below 6 pJ.

to screening of the internal field (dark electric field) between the finger electrodes by the space-charge field created by the field-induced separation of photogenerated electrons and hole at high illumination conditions.<sup>9,11,12</sup> The

measured FWHM's under a different optical energy are plotted in the inset of Fig. 93.41. As can be seen, the FWHM remains flat (60 ps) for optical energy up to 6 pJ, after which the FWHM increases by approximately 10 ps up to 110 pJ and then to 166 ps for optical energy of 391 pJ. The condition on which the space-charge effect does not affect the pulse shape of impulse response was calculated in Refs. 11 and 12 and given as

$$E < \frac{\epsilon_0(\epsilon_s + 1)L^2V(t + D)hc}{4\lambda qt^2(1 - r)[1 - \exp(-\alpha d)]}, \quad (1)$$

where  $E$  is the incident optical pulse energy,  $\epsilon_s$  is the relative permittivity of the semiconductor,  $L^2$  is the active area,  $V$  is the applied bias,  $t$  is the finger width,  $D$  is the interelectrode spacing,  $\lambda$  is the incident wavelength,  $r$  is the reflection coefficient,  $\alpha$  is the optical absorption coefficient, and  $d$  is the thickness of the GaN film. Based on all the parameters used in fabrication and experiment, we obtained a pulse energy of 6.54 pJ for our devices. This is in close agreement with our experimental results (FWHM starts increasing after 6 pJ).

In summary, MSM photodiodes have been fabricated on GaN with finger width and pitch ranging from 0.3  $\mu\text{m}$  to 5  $\mu\text{m}$ , and the impulse responses have been measured at  $\lambda = 270$  nm under both low and high illumination conditions with a fast, broadband circuit. For an optical pulse energy less than 6 pJ, the response speed of the detectors was about 60 ps, regardless of the bias voltages (up to 10 V) and finger dimensions. Analysis of the rise and fall times indicates that the very short photogenerated electric pulse was broadened by the measurement system. The inherent device response was determined to be less than 26 ps by the double-pulse measurements. At higher incident optical energies, the pulse width increased significantly due to the screening of the dark electric field between the finger electrodes. The experimental results are in close agreement with theory.

#### ACKNOWLEDGMENT

One of the authors (JL) thanks Ms. Lu Chen for her help at CNF. This work was supported by the U.S. Department of Energy Office of Inertial Confinement Fusion under Cooperative Agreement No. DE-FC03-92SF19460, the University of Rochester, and the New York State Energy Research and Development Authority. The support of DOE does not constitute an endorsement by DOE of the views expressed in this article.

## REFERENCES

1. R. P. Joshi, A. N. Dharamsi, and J. McAdoo, *Appl. Phys. Lett.* **64**, 3611 (1994).
2. J. C. Carrano *et al.*, *J. Electron. Mater.* **28**, 325 (1999).
3. J. C. Carrano *et al.*, *Appl. Phys. Lett.* **73**, 2405 (1998).
4. D. Walker *et al.*, *Appl. Phys. Lett.* **74**, 762 (1999).
5. T. Palacios *et al.*, *Appl. Phys. Lett.* **81**, 1902 (2002).
6. TDI, Inc., Silver Spring, MD 20904.
7. B. C. Wadell, *Transmission Line Design Handbook* (Artech House, Boston, 1991).
8. N. Biyikli *et al.*, *Appl. Phys. Lett.* **79**, 2838 (2001).
9. K. Aliberti *et al.*, *Appl. Phys. Lett.* **80**, 2848 (2002).
10. The details will be reported in a subsequent publication.
11. S. V. Averine and R. Sachot, *Solid-State Electron.* **44**, 1627 (2000).
12. S. V. Averine and R. Sachot, *IEE Proc., Optoelectron.* **147**, 145 (2000).